

<https://helda.helsinki.fi>

Increased Heparanase Levels in Urine during Acute Puumala Orthohantavirus Infection Are Associated with Disease Severity

Cabrera, Luz E.

Multidisciplinary Digital Publishing Institute
2022-02-22

Cabrera, L.E.; Schmotz, C.; Saleem, M.A.; Lehtonen, S.; Vapalahti, O.; Vaheri, A.; Mäkelä, S.; Mustonen, J.; Strandin, T. Increased Heparanase Levels in Urine during Acute Puumala Orthohantavirus Infection Are Associated with Disease Severity. *Viruses* 2022, 14, 450.

<http://hdl.handle.net/10138/349242>

Downloaded from Helda, University of Helsinki institutional repository.






This is an electronic reprint of the original article.

This reprint may differ from the original in pagination and typographic detail.

Please cite the original version.

Article

Increased Heparanase Levels in Urine during Acute Puumala Orthohantavirus Infection Are Associated with Disease Severity

Luz E. Cabrera ^{1,*}, Constanze Schmotz ², Moin A. Saleem ³, Sanna Lehtonen ^{2,4}, Olli Vapalahti ^{1,5,6}, Antti Vaheri ¹, Satu Mäkelä ^{7,8}, Jukka Mustonen ^{7,8} and Tomas Strandin ¹

- ¹ Department of Virology, Medicum, University of Helsinki, 00290 Helsinki, Finland; olli.vapalahti@helsinki.fi (O.V.); antti.vaheri@helsinki.fi (A.V.); tomas.strandin@helsinki.fi (T.S.)
- ² Research Program for Clinical and Molecular Metabolism, University of Helsinki, 00290 Helsinki, Finland; constanze.schmotz@helsinki.fi
- ³ Bristol Renal, Translational Health Sciences, Bristol Medical School, University of Bristol, Bristol BS1 3NY, UK; m.saleem@bristol.ac.uk
- ⁴ Department of Pathology, University of Helsinki, 00290 Helsinki, Finland; sanna.h.lehtonen@helsinki.fi
- ⁵ Virology and Immunology, Diagnostic Center, Helsinki University Hospital (HUSLAB), 00290 Helsinki, Finland
- ⁶ Department of Veterinary Biosciences, University of Helsinki, 00290 Helsinki, Finland
- ⁷ Department of Internal Medicine, Tampere University Hospital, Elämänaukio 2, 33520 Tampere, Finland; satu.makela@pshp.fi (S.M.); jukka.mustonen@tuni.fi (J.M.)
- ⁸ Faculty of Medicine and Health Technology, Tampere University, 33014 Tampere, Finland
- * Correspondence: Luz.cabreralara@helsinki.fi



Citation: Cabrera, L.E.; Schmotz, C.; Saleem, M.A.; Lehtonen, S.; Vapalahti, O.; Vaheri, A.; Mäkelä, S.; Mustonen, J.; Strandin, T. Increased Heparanase Levels in Urine during Acute Puumala Orthohantavirus Infection Are Associated with Disease Severity. *Viruses* **2022**, *14*, 450. <https://doi.org/10.3390/v14030450>

Academic Editor: William C. Wilson

Received: 19 January 2022

Accepted: 19 February 2022

Published: 22 February 2022

Publisher's Note: MDPI stays neutral with regard to jurisdictional claims in published maps and institutional affiliations.



Copyright: © 2022 by the authors. Licensee MDPI, Basel, Switzerland. This article is an open access article distributed under the terms and conditions of the Creative Commons Attribution (CC BY) license (<https://creativecommons.org/licenses/by/4.0/>).

Abstract: Old–world orthohantaviruses cause hemorrhagic fever with renal syndrome (HFRS), characterized by acute kidney injury (AKI) with transient proteinuria. It seems plausible that proteinuria during acute HFRS is mediated by the disruption of the glomerular filtration barrier (GFB) due to vascular leakage, a hallmark of orthohantavirus–caused diseases. However, direct infection of endothelial cells by orthohantaviruses does not result in increased endothelial permeability, and alternative explanations for vascular leakage and diminished GFB function are necessary. Vascular integrity is partly dependent on an intact endothelial glycocalyx, which is susceptible to cleavage by heparanase (HPSE). To understand the role of glycocalyx degradation in HFRS–associated proteinuria, we investigated the levels of HPSE in urine and plasma during acute, convalescent and recovery stages of HFRS caused by Puumala orthohantavirus. HPSE levels in urine during acute HFRS were significantly increased and strongly associated with the severity of AKI and other markers of disease severity. Furthermore, increased expression of HPSE was detected in vitro in orthohantavirus–infected podocytes, which line the outer surfaces of glomerular capillaries. Taken together, these findings suggest the local activation of HPSE in the kidneys of orthohantavirus–infected patients with the potential to disrupt the endothelial glycocalyx, leading to increased protein leakage through the GFB, resulting in high amounts of proteinuria.

Keywords: Puumala hantavirus; acute kidney injury; proteinuria; glycocalyx; podocytes; heparanase; syndecan–1

1. Introduction

Orthohantaviruses are zoonotic pathogens able to cause two major clinical syndromes: hemorrhagic fever with renal syndrome (HFRS) and hantavirus cardiopulmonary syndrome (HCPS). Different orthohantavirus species possess varying pathogenicity in humans. The prototype orthohantavirus Hantaan (HTNV, circulates in Eastern Asia) causes a more severe form of HFRS with mortality up to 5%, whereas Puumala orthohantavirus (PUUV, mainly in Northern Europe) causes a mild form of the disease often referred to as nephropathia

epidemia (NE, mortality 0.1%). Orthohantaviruses circulating in the Americas are associated with the highly severe HCPS (mortality > 30%) [1]. HFRS is characterized by changes in the endothelial barrier functions, fluid alterations including extravasation, increased glomerular permeability and proteinuria [2–4].

Renal involvement in acute NE includes transient proteinuria, microscopic hematuria, and oliguric acute kidney injury (AKI). This is followed by a polyuric phase and finally recovery [4]. Proteinuria in NE is mostly composed of albumin, but larger proteins such as IgG are also found in the urine, suggesting proteinuria to have a glomerular origin [5]. Albuminuria makes a flash-like appearance and returns rapidly to normal levels in 2–3 weeks [6], and the amount of this albuminuria on admission to hospital predicts the severity of upcoming AKI [7]. Additionally, a concomitant urinary loss of low-molecular-weight proteins such as β_2 - and α_1 -microglobulin indicates that tubular injury also contributes to the proteinuria. A typical renal biopsy finding is acute tubulointerstitial nephritis with only minor glomerular light microscopic abnormalities. The glomerular barrier breakdown seems to be caused by the release of cytokines and other vasoactive factors, rather than by endothelial cell death [4]. By electron microscopy, however, podocyte foot-process effacement has been documented [8].

AKI, an acute decline in glomerular filtration rate (GFR) determined by elevated serum creatinine levels, is found in most hospital-treated patients in Finland [4] and presents with a favorable outcome [9].

The functional structure in the kidney preventing the excretion of large plasma proteins into the urine is known as the glomerular filtration barrier (GFB). The GFB is composed of pedicles of podocytes, the glomerular basement membrane, and the glomerular endothelium of capillaries [10]. The active role that the glomerular endothelium plays in renal filtration is linked to its negatively charged surface of proteoglycan glycosaminoglycans (GAG) and glycoprotein molecules: the glycocalyx [11–15]. It acts by preventing negatively charged molecules of similar or larger size than albumin to be excreted through the urine, a process known as charge selectivity [16]. Importantly, the increased glomerular permeability seen in PUUV-HFRS was demonstrated to be associated with impairment of the size- and charge-selectivity properties of the GFB [5]. Interestingly, orthohantaviruses can infect different cells of the human kidney, including glomerular endothelial cells, tubular epithelial cells, and podocytes, resulting in the disruption of their cell-to-cell interactions [17,18]. Furthermore, recent findings suggest podocyte injury to be the main cause of proteinuria in PUUV-HFRS [19].

Damage to the endothelial glycocalyx has been implicated in vascular permeability, one of the major pathophysiological aspects of orthohantaviral diseases [20]. Therefore, it is necessary to study the possibility of the enzymatic destruction of these endothelial components, which has been demonstrated to result in increased urinary excretion of albumin in previous studies [21–25].

The function of heparan sulfate (HS), the major GAG component [26–29], is regulated by active heparanase (HPSE), which cleaves HS on its polymeric chains and internal sites [30]. Studies performed on mice demonstrated the importance of GAGs in renal charge selectivity [31] and the effect of HPSE in degrading the volume fraction of negatively charged fibers in the glycocalyx [22]. Similarly, syndecan-1 is a heparan sulfate proteoglycan (HSPG) present on the surfaces of endothelial cells. In addition to the cleavage of syndecan-1 HS side chains, HPSE also promotes the cleavage and release of its biologically active ectodomain. Thus, syndecan-1 is a renowned marker of glycocalyx degradation [32–34]. Moreover, syndecan-1 is known to bind to many mediators of disease pathogenesis [35] and, strikingly, it has been found to be elevated in the circulating blood during PUUV-HFRS, where syndecan-1 levels associated with albumin levels and vascular leakage parameters, as well as disease severity [36].

The aim of this study is to investigate the mechanisms of glycocalyx degradation during PUUV infection by determining the concentration of HPSE in the plasma and urine

of PUUV-infected patients, as well as in orthohantavirus-infected human kidney cells, to better understand the underlying physiopathological processes during acute PUUV-HFRS.

2. Materials and Methods

2.1. Ethics Statement and Clinical Samples

The Ethics Committees of Tampere University Hospital (permit number R04180) approved the use of patient samples. All subjects gave written informed consent in accordance with the Declaration of Helsinki. The study material consisted of plasma and urine from hospitalized, serologically confirmed acute PUUV infection at Tampere University Hospital, Finland, between 2005 and 2009. The samples were collected sequentially during acute (hospitalization) and convalescent (20–30 days after onset of fever) phases, as well as 6 months and one year after full recovery, used as controls. Sequential samples included plasma as well as urine from 56 patients (Table 1). The samples were stored at -80°C prior to analysis. Urinary creatinine was determined by an Atellica CH5 analyzer (Siemens; Berlin, Germany) at the Helsinki and Uusimaa Hospital District diagnostic laboratory. Daily white blood cell (WBC), plasma C-reactive protein (CRP) and serum creatinine concentrations were determined at the Laboratory Centre of the Pirkanmaa Hospital District (Tampere, Finland) using standard methods. Daily urine creatinine and albumin concentrations were determined at the University of Massachusetts Memorial Health Care Hospital Labs using standard methods [6]. The estimated glomerular filtration rate (eGFR) was calculated using the Chronic Kidney Disease Epidemiology Collaboration (CKD-EPI) equation [37].

Table 1. Clinical and laboratory parameters of PUUV-HFRS patients. Abbreviations: eGFR = estimated glomerular filtration rate, HPSE = heparanase, IL = interleukin, IP-10 = interferon gamma-induced protein-10, MCP-1 = monocyte chemoattractant protein-1, MPO = myeloperoxidase.

Variable (Unit)	Mean (SE; Range)
Number of patients	56
Hospital length of stay (days)	5.81 (0.46; 2–25)
Age (years)	41 (1.65; 22–73)
Male: Female ratio	2.3:1
Min eGFR (mL/min/1.73m ²)	63 (5.75; 5–141)
Max plasma creatinine (μmol/L)	266.22 (35.61; 45–1071)
Urine albumin: creatinine ratio (mg/g)	1012.12 (190.67; 2.9–5530.8)
Max urine HPSE: creatinine ratio (mg/g)	0.22 (0.04; 0–1.17)
Min plasma albumin (g/dL)	2.41 (0.08; 2.3–3.5)
Max plasma HPSE (ng/mL)	4.54 (0.70; 0–20.23)
Max urine syndecan-1: creatinine ratio	36.3 (9.5; 0–411.62)
Urine IL-6: creatinine ratio (pg/μg)	0.21 (0.05; 0.005–1.30)
Plasma IL-6 (pg/mL)	128.58 (39.9; 10–785.8)
Urine IL-8: creatinine ratio (pg/μg)	0.45 (0.18; 0.003–5.80)
Plasma IL-8 (pg/mL)	41.26 (8.72; 10–234.86)
Urine IP-10: creatinine ratio (pg/μg)	4.47 (0.70; 0.22–16.92)
Plasma IP-10 (pg/mL)	4734.39 (764.17; 739.8–18224)
Urine MCP-1: creatinine ratio (pg/μg)	7.64 (1.97; 0.01–63.64)
Plasma MCP-1 (pg/mL)	373.97 (120.78; 23.5–3636.78)
MPO (ng/mL)	150.85 (9.5; 46–332.17)
Severity score	4.04 (0.24; 0–7)
Min mean arterial pressure (mmHg)	84.11 (1.42; 51.33–103.33)
Max CRP (mg/L)	67.32 (5.11; 9.7–155.2)
Min thrombocytes (10 ⁹ /L)	85.56 (5.66; 36–266)
Max leukocytes (10 ⁹ /L)	10.62 (0.58; 4.1–25.5)

The overall severity of patients was assessed by a score system adapted from the sequential organ failure assessment scoring system, where the maximum levels of plasma creatinine (4 = >440, 3 = 300–440, 2 = 171–299, 1 = 110–170 and 0 = <110 μmol/L), minimum level of thrombocytes (4 = <20, 3 = 20–49, 2 = 50–99, 1 = 100–150 and 0 = >150 × 10⁹/L)

and lowest mean arterial blood pressure (MAP) measured during hospitalization (1 = <70 and 0 = ≥70 mmHg) were ranked.

2.2. HPSE Measurement Assay

HPSE levels from patient samples and cell culture supernatants were measured through the enzyme's ability to cleave HS, which was quantified with the use of a standard curve, as described in [38]. In detail, Nunc maxisorp flat-bottom 96-well plates (Thermo scientific; Breda, The Netherlands) were coated with 10 µg/mL heparan sulfate from bovine kidney (HSBK) (Sigma-Aldrich; Zwijndrecht, The Netherlands) in coating buffer (3.3 M ammonium sulfate ((NH₄)₂SO₄)), for 1 h at 37 °C. Subsequently, plates were washed with PBS supplemented with 0.05% Tween 20 (PBST) and blocked with 1% BSA in PBS at RT. After blocking, plates were washed with PBST, followed by a final washing step with PBS. Plasma and urine samples were then incubated for 2 h at 37 °C, in a 1:4 dilution in HPSE buffer (50 mM citric acid–sodium citrate, 50 mM NaCl, 1 mM CaCl₂ at pH 5.0). Next, plates were washed with PBST and incubated with primary mouse anti-rat IgM HS antibody JM403 (Amsbio; Abingdon, United Kingdom, cat. no. #370730-S, RRID: AB_10890960, 1 µg/mL in PBST) for 1 h at RT, washed with PBST and then incubated with secondary goat anti-mouse IgM HRP antibody (Southern Biotech; Uden, The Netherlands, cat. no. #1020-05, RRID: AB_2794201, 1:10,000 dilution in PBST) for 1 h at RT and washed with PBST once again. Finally, 3,3',5,5'-tetramethylbenzidine (TMB) substrate (Sigma-Aldrich, Zwijndrecht, The Netherlands) was added to the plates, the reaction was stopped by the addition of 0.5 M sulfuric acid, and absorbance was measured at 450 nm. The HPSE concentration in the plasma and urine of patient samples, as well as from podocyte cultures, was compared to a standard curve of recombinant human HPSE (Bio-technie; Abingdon, UK, Cat#7570-GH-005). Urine concentrations measured were then normalized by dividing the values by creatinine (heparanase:creatinine ratio).

2.3. ELISAs

The syndecan-1 ELISA kit was purchased from R&D Systems and used according to the manufacturer's protocol (Human Syndecan-1 DuoSet, Catalog no. DY2780; Bio-technie; Abingdon, UK). Cytokines interleukin (IL)-6, IL-8, monocyte chemoattractant protein (MCP)-1 and interferon-gamma induced protein (IP)-10 were measured previously from plasma and urine by Luminex [39]. Myeloperoxidase (MPO) was measured from plasma previously [40]. The concentrations measured in urine were normalized by dividing the values by creatinine (syndecan-1:creatinine ratio, IL-6:creatinine ratio, IL-8:creatinine ratio, IP-10:creatinine ratio, MCP-1:creatinine ratio).

2.4. Virus Isolates

The PUUV-Suonenjoki (PUUV-Suo) strain was propagated in a bank vole renal epithelial cell line (MyGlaRec.B from EVAg), grown in Dulbecco's minimum essential medium—high glucose (DMEM; Sigma Aldrich; Zwijndrecht, The Netherlands) supplemented with 10% inactivated FCS, 100 IU/mL penicillin, 100 µg/mL streptomycin, 2 mM L-glutamine and a mix of non-essential amino acids (Sigma Aldrich; Zwijndrecht, The Netherlands). The HTNV strain 76-118 was grown in Vero E6 cells (green monkey kidney epithelial cell line; ATCC no. CRL-1586) in Minimum Essential Medium (MEM; Sigma-Aldrich; Zwijndrecht, The Netherlands) and supplemented with 10% inactivated FCS, 100 IU/mL of penicillin and 100 µg/mL of streptomycin and 2 mM of L-glutamine. Viruses were purified from cell culture supernatants by ultracentrifugation through a 30% sucrose cushion (SW28 rotor, 27,000 rpm, 50 min, +4 °C) and suspended to the corresponding growth medium. The infectious titers of PUUV and HTNV stocks were routinely 10⁵ and 10⁷ focus-forming units (FFU)/mL, respectively. Virus titers were measured by incubating diluted virus stocks with Vero E6 cells for 24 h at 37 °C, followed by acetone fixation and staining with a rabbit polyclonal antibody specific for PUUV nucleocapsid (N) protein (anti-PUUN) and AlexaFluor488-conjugated donkey anti-rabbit secondary

antibody (Thermo Scientific; Breda, The Netherlands). Fluorescent focus-forming units (FFFU)/mL were counted under a UV microscope (Zeiss Axio Imager 1; Zeiss, Jena, Germany). Where indicated, viruses were inactivated using UV crosslinker (300,000 $\mu\text{J}/\text{cm}^2$, Stratalinker, Stratagene).

2.5. Podocyte Cultures

Conditionally immortalized human podocytes (AB 8/13) [41] were cultured in RPMI-1640 growth medium supplemented with 10% fetal calf serum (FCS) and 1% ITS (Sigma-Aldrich; Zwijndrecht, The Netherlands), maintained at 33 °C and shifted to 37 °C for differentiation, on Viewplate black 96-well plates (PerkinElmer, Inc; Waltham, MA, USA). At 8 days of differentiation, podocyte cultures were infected with UV-inactivated or live virus isolates at the indicated multiplicity of infection (MOI) for 1 h at 37 °C, after which the virus-containing medium was changed back to podocyte growth medium. At indicated days post-infection (dpi), supernatants were collected and frozen in -20 °C and cells were washed with PBS prior to fixation with 4% paraformaldehyde (PFA) for 10 min.

2.6. Immunofluorescence

The podocyte infection frequency was assessed by staining permeabilized (PBS supplemented with 3% BSA and 0.1% TritonX-100 for 10 min) cells with anti-PUUN rabbit serum followed by AlexaFluor488-conjugated secondary antibody (Thermo Scientific; Breda, The Netherlands) supplemented with 1:5000 diluted Hoechst 33420. Finally, imaging was performed with a PerkinElmer Opera Phenix (PerkinElmer, Inc; Waltham, MA, USA) spinning disk confocal microscope using a 5 \times water-immersion objective (NA 1.0). The analysis of the number of infected cells was conducted with the Harmony software (PerkinElmer, Inc; Waltham, MA, USA) by using a supervised linear classifier.

2.7. HPSE mRNA Expression

The expression of HPSE mRNA was determined from RNA isolated from podocytes ($n = 2$ for each infection group and time point) using Trizol according to the manufacturer's instructions (Thermo Scientific; Breda, The Netherlands). The expression of HPSE and GAPDH mRNAs was quantified by one-step reverse-transcriptase quantitative polymerase chain reaction (RT-qPCR) with commercial FAM- and VIC-based fluorescent primer-probe sets (Thermo Scientific; Breda, The Netherlands), respectively, employing 1-step fast virus master mix (Thermo Scientific; Breda, The Netherlands) and AriaMx real-time PCR instrumentation (Agilent, Santa Clara, CA, USA). The relative expression of HPSE mRNA was calculated by the $2^{-\Delta\Delta\text{Ct}}$ method [42] using GAPDH for normalization and the average of mock samples ($n = 4$) as a reference.

2.8. Statistical Analysis

Statistical analysis was performed using GraphPad Prism 8.3 software (GraphPad Software; San Diego, CA, USA), R software v3.6.3 (R core team) and SPSS v25 (IBM; Armonk, NY, USA). Statistically significant differences between groups were assessed with Kruskal-Wallis or Tukey's multiple comparisons test, depending on the sample distribution and the number of groups analyzed. Statistically significant correlations between normally and non-normally distributed variables were assessed by calculating Spearman's correlation coefficients. Following rank transformation of non-normally distributed variables, normality was assessed with Anderson-Darling, D'Agostino-Pearson omnibus, Shapiro-Wilk and Kolmogorov-Smirnov tests. Then, the correlations between variables were examined using the Pearson's correlation coefficient test to confirm that multicollinearity between variables did not exist, to conduct simple and linear regression analyses. Statistically significant differences during various time points after the onset of fever (aof), using the last convalescence time point (365 days aof) as the reference category, were assessed by generalized estimating equations (GEE), assuming a linear distribution and setting the working correlation matrix to independent.

3. Results

3.1. HPSE and Syndecan-1 Levels Are Increased in Urine of Acute PUUV-HFRS Patients

In support of potential glycocalyx degradation during acute PUUV-HFRS, HPSE and syndecan-1 concentrations were significantly increased in urine samples collected from patients during the acute (days aof 3–9) phase of PUUV-HFRS, compared to the convalescence (days aof 20–30) and control phase (182 and 365 aof) (Figure 1A,B). The elevated levels of urinary HPSE and syndecan-1 coincided with increased levels of albumin in urine during the acute stage of the disease (Figure 1C). However, plasma HPSE in the acute phase was not elevated, as compared to the control phase (Figure 1D). Taken together, these findings suggest that if HPSE affects endothelial glycocalyx degradation during PUUV-HFRS, its effect is exerted locally in the kidneys, rather than systemically.

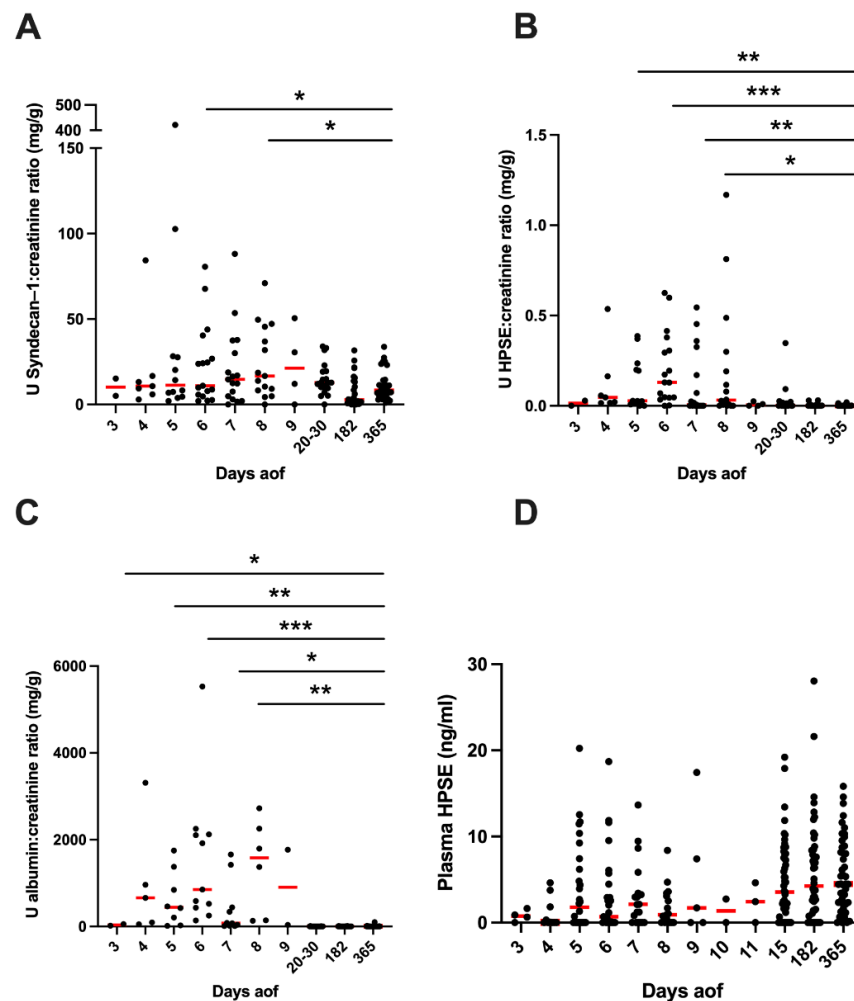


Figure 1. Heparanase and syndecan-1 levels during PUUV-HFRS. (A) Urinary syndecan-1:creatinine ratio (B), HPSE:creatinine ratio and (C) albumin:creatinine ratio. (D) HPSE concentration in plasma. Concentrations were measured from sequential samples of 49 (55 for plasma) patients hospitalized due to PUUV-HFRS (with a total of 159 urine and 262 plasma samples). Days after onset of fever (aof) 3–9 represent the acute stage, 20–30 the convalescent and 182–365 the controls. Differences between individual time points and the last time point (365 aof), which was considered to represent full recovery and used as controls, were assessed by GEE and significant differences indicated as *** < 0.001 , ** < 0.01 and * < 0.05 . Red lines represent mean \pm standard deviation.

3.2. Urinary HPSE Levels Correlate with Albuminuria and Other Disease Severity Markers

Next, we considered whether there was a link between HPSE, syndecan-1 and albumin measured from urine, as well as their association with different inflammatory cytokines

and chemokines measured previously from the same set of patients, and clinical parameters describing the severity of this disease. Significant bivariate associations were assessed by calculating Spearman's rank correlation coefficients (Figure 2), and urinary HPSE showed a significant positive correlation with urinary albumin levels ($p < 0.0001$, $r = 0.734$), followed by overall disease severity evaluated with the severity score ($p = 0.007$, $r = 0.394$). Additionally, HPSE in urine was significantly higher in patients with a lower eGFR, the hallmark of AKI ($p = 0.046$, $r = -0.299$). Albuminuria did, however, show a significant positive correlation with urinary interleukin 6 ($p = 0.049$, $r^2 = 0.340$), an inflammatory cytokine directly leaking from plasma to urine, as well as with total blood leukocyte counts ($p = 0.015$, $r^2 = 0.368$) and granulocyte-derived myeloperoxidase (MPO) levels in circulating blood ($p = 0.010$, $r^2 = 0.381$). In contrast, urinary HPSE did not show significant correlations with these parameters. Thus, the lack of association between urinary HPSE and markers of systemic inflammation points towards the local expression of HPSE in the kidneys of acute PUUV-HFRS. As for urinary syndecan-1, its levels displayed a significant positive correlation with the pro-inflammatory plasma IL-6 ($p = 0.011$, $r^2 = 0.439$), IL-8 ($p = 0.002$, $r^2 = 0.512$) and MCP-1 ($p = 0.010$, $r^2 = 0.44$) levels. In addition to the correlations shown in Figure 2, in which urine values were normalized with urinary creatinine levels, correlations using the absolute urinary concentrations were also assessed (Supplementary Figure S1). The significant associations of urinary HPSE and syndecan-1 with other parameters tested were essentially the same and generally with increased p -values.

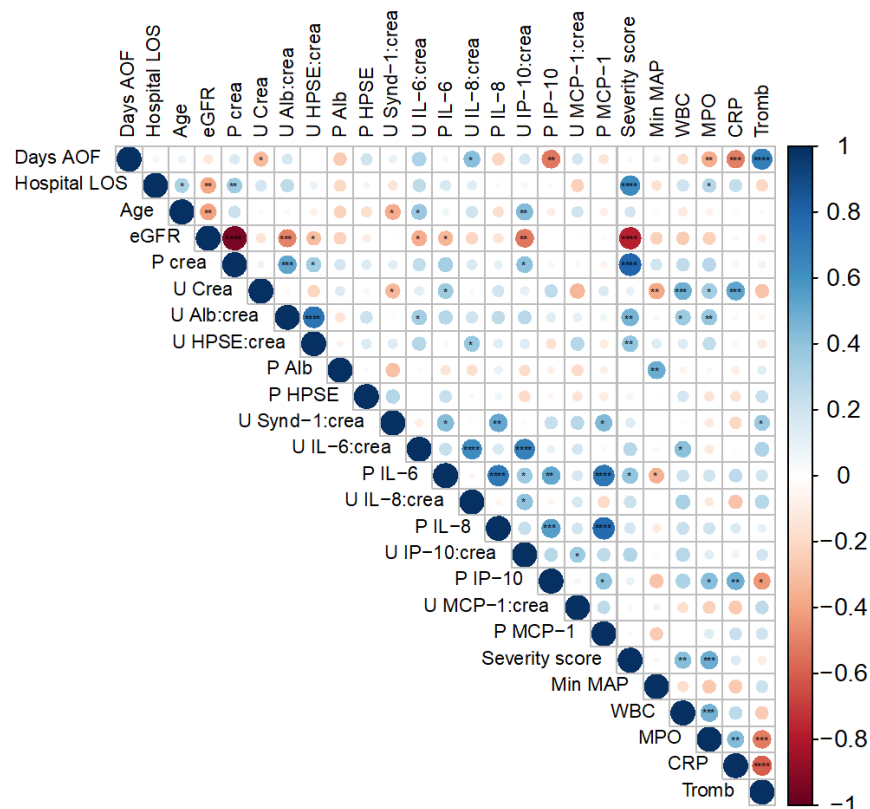


Figure 2. Spearman's rank correlation coefficient matrix. The colors of the round circles indicate the level of the correlation coefficient and increasing size with a lower p -value. Statistical significance is specified as * = $p < 0.05$, ** = $p < 0.01$, *** = $p < 0.001$, **** = $p < 0.0001$. AOF = after onset of fever, LOS = length of stay, eGFR = estimated glomerular filtration rate, P = plasma, U = urine, crea = creatinine, alb = albumin, HPSE = heparanase, Synd-1 = syndecan-1, IL = interleukin, IP-10 = interferon gamma-induced protein 10, MCP-1 = monocyte chemoattractant protein 1, min MAP = minimum mean arterial pressure, WBC = white blood cells, MPO = plasma myeloperoxidase, CRP = plasma C-reactive protein, tromb = blood thrombocytes.

3.3. Urinary HPSE Levels Possess Predictive Power over Disease Severity, Albuminuria and Hypotension

Following the assessment of significant correlations between different parameters, we wished to investigate the possible predictive power between urinary HPSE and other variables of interest. For this purpose, we initially performed single regression models of urinary albumin and urinary HPSE levels as predictors of disease severity, assessed with a severity score, and found both to explain severity to various degrees: urinary albumin levels could explain 19% of the variability in disease severity ($p = 0.0025$, $r^2 = 0.1934$); meanwhile, urinary HPSE could account for 13% of the variability in the severity score ($p = 0.0132$, $r = 0.1346$) (Figure 3A,B, Table 2).

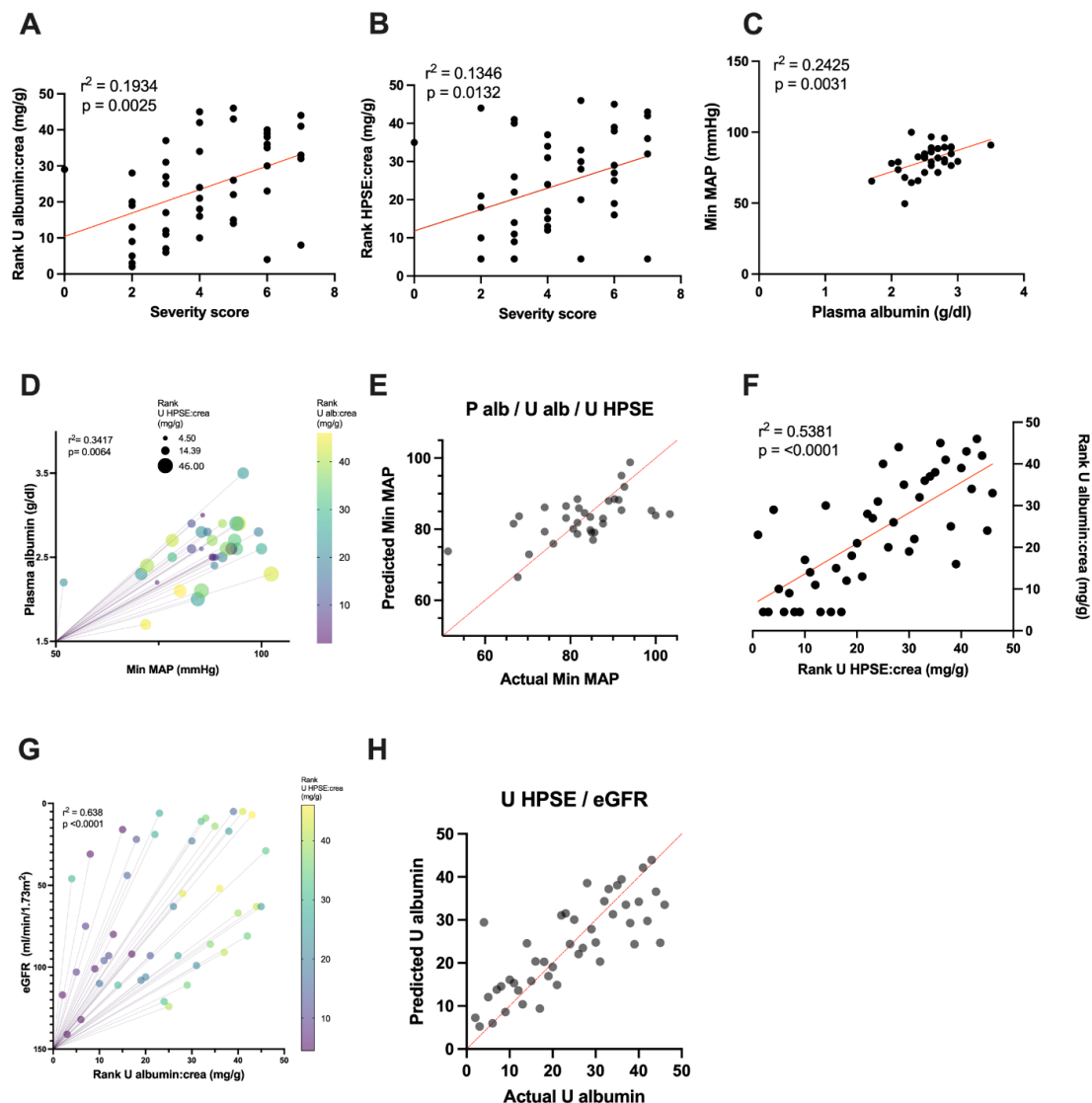


Figure 3. Simple and multiple linear regression models. Simple linear regression models of rank-transformed urinary albumin:creatinine ratio (A) and rank-transformed urinary HPSE:creatinine ratio (B) with severity score. (C) Simple linear regression model of plasma albumin and MAP. (D) Multiple linear regression model of plasma albumin, rank-transformed urinary HPSE:creatinine ratio and rank-transformed albumin on MAP. (E) Predicted vs. actual MAP of multiple linear regression model in (D). (F) Simple linear regression model of rank-transformed urinary HPSE:creatinine ratio and albumin:creatinine ratio. (G) Multiple linear regression model of eGFR and urinary HPSE on albuminuria. (H) Predicted vs. actual data of the multiple regression model in (G).

Table 2. Simple and multiple regression models.

Dependent Variables	Type of Regression	Independent Variables	Estimate	Std. Error	95% CI	t Value	p-Value of Variable	R ²	F-Statistic	p-Value of Model
Minimum mean arterial pressure	Simple	Plasma albumin	15.594	4.715	[5.488–24.7]	3.440	0.0031 **	0.2425	10.25	0.0031 **
	Multiple	Plasma albumin	15.4735	4.8731	[5.507–25.44]	3.175	0.0035 **	0.3417	5.017	0.0064 **
		Urinary albumin: creatinine ratio	−0.1508	0.1774	[−0.5136–0.2121]	−0.85	0.0724			
		Urinary HPSE: creatinine ratio	0.3703	0.1854	[−0.0088–0.7495]	1.998	0.0502			
Severity score	Simple	Urinary albumin: creatinine ratio	3.254	1.014	[1.210–5.299]	3.211	0.0025 **	0.1934	10.31	0.0025 **
	Simple	Urinary HPSE: creatinine ratio	2.799	1.082	[0.6167–4.982]	2.586	0.0132 *	0.1346	6.690	0.0132 *
Urinary albumin: creatinine ratio	Simple	Urinary HPSE: creatinine ratio	0.7355	0.1027	[0.5257–0.9376]	0.1027	<0.0001 ***	0.5276	51.26	<0.0001 ***
	Multiple	Urinary HPSE: creatinine ratio	0.6587	0.0941	[0.4687–0.8486]	6.998	<0.0001 ***	0.621	37.02	<0.0001 ***
		eGFR	−0.0848	0.0308	[−0.1469–−0.0227]	−2.756	0.0086 **			

Statistical significance is specified as * = $p < 0.05$, ** = $p < 0.01$, *** = $p < 0.001$.

To demonstrate the link between plasma albumin and the vasculature, we assessed the association between this circulating protein and the minimum mean arterial pressure (MAP) presented by patients during their hospital stay. Results exhibited a correlation between low MAP and a decreased plasma albumin concentration ($p = 0.003$, $r^2 = 0.492$) (Figure 2). Moreover, a linear regression model between these two variables confirmed their strong association ($p = 0.0031$, $r^2 = 0.2425$) (Figure 3C). Additionally, combining plasma albumin with other variables of relevance (HPSE in urine or plasma, albumin in urine and eGFR) in multiple regression analysis models revealed that the predictive power of plasma albumin on hypotension was strengthened only in the presence of both urinary HPSE and urinary albumin levels ($p = 0.0064$, $r^2 = 0.3417$) (Figure 3D,E), explaining up to 34% of the variability in blood pressure.

Following this discovery, we wished to assess the association between urinary HPSE and other parameters. We found, through simple linear regression analyses, that urinary HPSE was significantly linked to albuminuria ($p < 0.0001$, $r^2 = 0.5381$) (Figure 3F), but none of the other independent variables. Although eGFR was not significantly associated with urinary HPSE in a simple regression model, a multiple regression model showed that eGFR combined with urinary HPSE increased the predictive power on albuminuria, explaining up to 64% of its variability ($p < 0.0001$, $r^2 = 0.638$) (Figure 3G,H). However, eGFR did not increase the predictive power of urinary albumin on urinary HPSE levels to the same extent ($p < 0.0001$, $r^2 = 0.5773$) (not shown), accounting for 58% of the variability in urinary HPSE levels. Furthermore, removal of urinary HPSE from the multiple regression model produced a major drop in the variability prediction and significance to 30% ($p = 0.0063$, $r^2 = 0.3039$) (not shown).

3.4. Upregulation of HPSE in Orthohantavirus-Infected Podocytes

Orthohantaviruses have been shown to infect podocytes [17,18], which have been postulated as major contributors of HPSE during kidney diseases (e.g., diabetic nephropathy) [43,44]. To assess the ability of orthohantavirus infection to induce HPSE upregulation in podocytes, we infected conditionally immortalized and differentiated human podocytes with various amounts (high and low dose; MOI 10 and 1, respectively) of Hantaan orthohantavirus (HTNV). We analyzed virus infectivity and HPSE expression by comparing HTNV-infected cells with UV-inactivated HTNV (MOI 10) or mock-infected cells at 2 and 4 dpi (Figure 4). As judged by viral nucleocapsid N-specific intracellular immunofluorescence, we observed efficient infection only in cells infected with a high dose of HTNV (Figure 4A, ~70% of infected cells at both 2 and 4 dpi). Interestingly, in line with infection efficiency, we observed a significant increase in HPSE expression in podocyte supernatants infected with a higher viral dose, but not in those infected with a lower dose or UV-inactivated HTNV (Figure 4B). Consistently, we observed mildly but significantly increased expression of HPSE mRNA only in cells infected with high-dose HTNV (Figure 4C, ~1.5-fold over mock-infected cells), indicating that the increase in HPSE levels is most likely due to increased transcriptional activity.

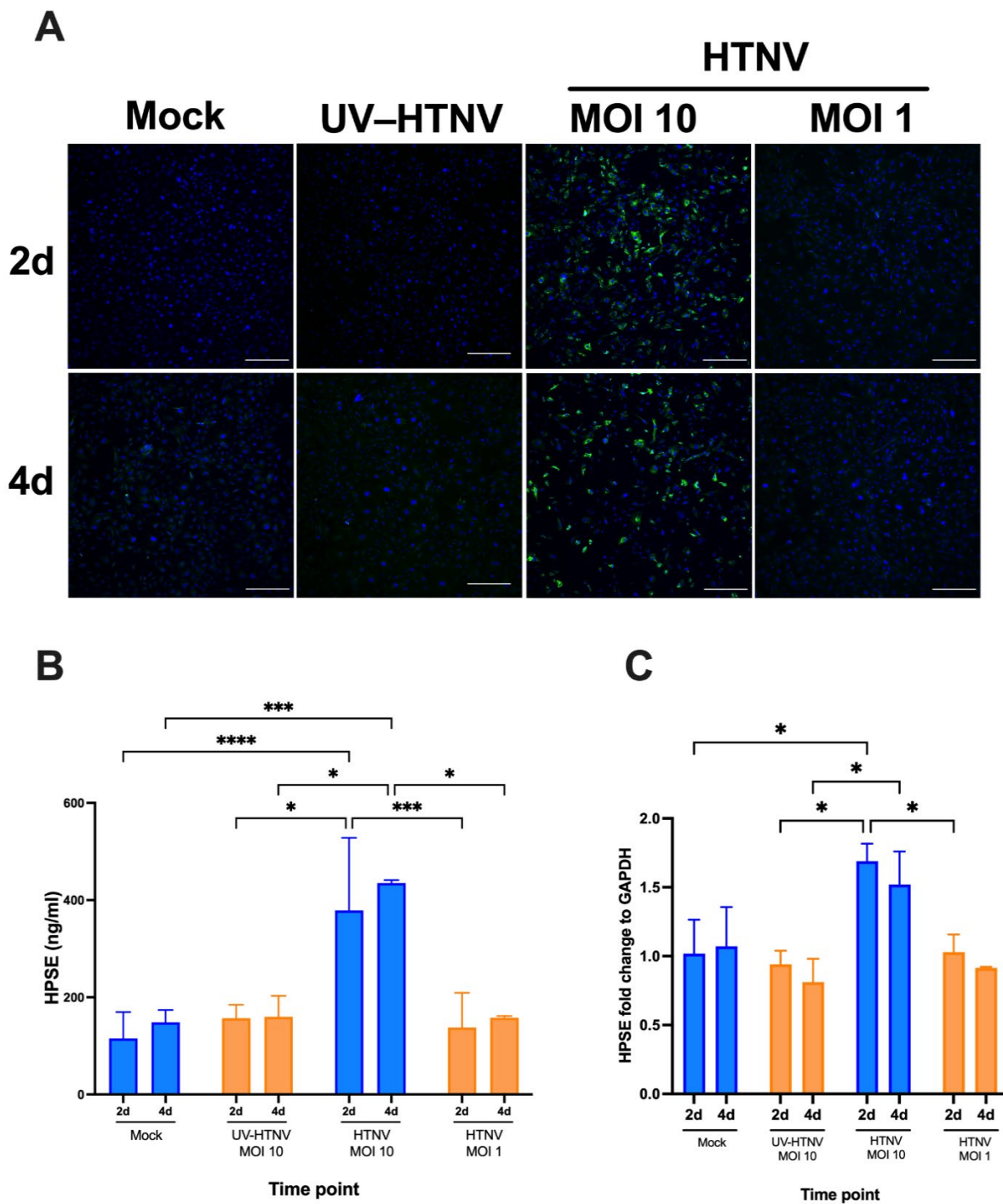


Figure 4. Increased HPSE concentration in HTNV-infected podocytes. Podocytes were infected with live HTNV (MOI 10 or 1), UV-inactivated HTNV (MOI 10) or remained uninfected (mock). Supernatants were collected and cells either fixed for immunofluorescence analysis or subjected to RNA extraction at 2 and 4 dpi. (A) Fixed and permeabilized podocytes were stained with rabbit serum against viral nucleocapsid N protein followed by AF488-conjugated secondary antibody (green) or Hoechst 33,420 to detect nuclei (blue). (B) HPSE levels measured from podocyte supernatants. (C) Isolated RNA was subjected to multiplex RT-qPCR with primers and probes detecting HPSE and GAPDH mRNA. The signal for HPSE mRNA was normalized based on GAPDH mRNA levels and fold change calculated in reference to mock-infected podocytes. Statistically significant differences were assessed with Tukey’s multiple comparisons test. ****, *** and * indicate $p < 0.0001$, $p < 0.001$ and $p < 0.05$, respectively.

4. Discussion

One of the major pathophysiological aspects of old-world orthohantaviral diseases is the presence of vascular leakage, an increased glomerular permeability linked to size- and charge-selectivity in the glomerular filtration barrier (GFB) and proteinuria. Since the disruption of the endothelial glycocalyx has been implicated as one of the potential mechanisms leading to vascular permeability, this study indirectly assessed endothelial damage through the measurement of the glycocalyx-degrading enzyme HPSE; and a well-known marker of glycocalyx degradation, syndecan-1, from the urine of PUUV-infected patients. Results showed significantly increased HPSE and syndecan-1 protein levels in patient urine during acute PUUV-caused HFRS compared to full recovery, used as a control. Additionally, these parameters significantly correlated with several important inflammatory markers describing disease severity and the extent of AKI: urinary syndecan-1 was associated with indicators of systemic inflammation (plasma IL-6, IL-8 and MCP-1), whereas urinary HPSE was linked to indicators of renal dysfunction (albuminuria, lower eGFR and higher plasma creatinine levels) and finally higher severity scores, representing a more severe overall clinical presentation. This association between urinary HPSE and disease severity was confirmed with a simple regression linear model, where HPSE explained up to 13% of the variability of the severity scores.

Syndecan-1 has been found to be elevated in the plasma of acute PUUV-HFRS in a previous study [36], and our results exhibited higher syndecan-1 levels in urine during acute disease. Interestingly, though, urinary syndecan-1 did not correlate with the same urinary parameters as HPSE. This difference could be due to its low molecular weight (30 kDa), which makes syndecan-1 more likely to be freely filtered through the glomerulus. While convalescent and recovery control phase samples presented significantly lower levels of syndecan-1 than during the acute infection, syndecan-1 was still detectable in control samples a year after the onset of disease (Figure 1A). It is possible that the epithelial cells of the urinary tract could also produce syndecan-1 into urine, as is the case for Tamm Horsfall protein [45]. Another possibility is a partial tubular reabsorption defect of syndecan-1, possibly resulting from a permanent tubular damage, as seen in some patients presenting with urinary long-lasting α 1-microglobulin levels after acute PUUV-HFRS infection [46,47]. HPSE, on the other hand, is an enzyme with a molecular weight of 50 kDa, not detected in control urine. Therefore, it is most likely not freely filtered nor reabsorbed. Thus, it is similar to albumin, the main plasma protein with a high molecular weight (66.5 kDa), known to bypass the GFB only under pathological conditions.

Altogether, these findings suggest that increased urinary HPSE and syndecan-1 are related to the damage of the renal structures and point towards a degradation of the endothelial glycocalyx during HFRS. This is supported by previous studies demonstrating HPSE as a player in kidney damage and dysfunction, including other renal pathologies that present proteinuria [48–50].

Our data showed that patients with lower plasma albumin levels presented significantly more severe hypotension during their hospital stay (minimum levels of MAP) ($p = 0.0031$, $r = 0.2425$), with plasma albumin explaining 24% of the variability in blood pressure. Moreover, the combination of plasma albumin concentration with urinary HPSE and albumin in multiple regression analysis models increased the predictability of hypotension by 10%. Additionally, the subtraction of urinary HPSE from the models resulted in no change in the predictive power of plasma albumin in MAP, together with a decrease in the statistical power ($p = 0.013$ and $r^2 = 0.24$ in both cases), compared to the simple regression model from Figure 3D.

Subsequently, the association between urinary HPSE and albuminuria was modeled in a simple linear regression analysis. This model was significant and displayed urine HPSE explaining up to 54% of the variability of urine albumin. When combined with eGFR, the predictability of urinary HPSE in albuminuria increased to 64%. Overall, the presence of urinary HPSE was required for increasing the predictive power of the multiple

regressions modeled for MAP and albuminuria as dependent variables, and important clinical manifestations during HFRS.

Perhaps unexpectedly, the plasma HPSE concentration measured during acute PUUV–HFRS was not increased, but rather seemed somewhat decreased compared to control phase samples (Figure 1D). This can be explained by the leakage of this enzyme into the urine. However, the increased HPSE levels measured from the urine samples do not seem to depend only on this leakage, since plasma HPSE was found to positively correlate with urinary HPSE, albumin and protein. If plasma was the sole source of HPSE in urine, these two variables would present a negative correlation. Thus, these findings suggest an increased HPSE production and not mere relocalization between bodily fluids. In addition, since our HPSE assay measured the active enzyme concentration of HPSE, it is possible that the measured levels of plasma HPSE during acute HFRS were affected by the presence of circulating HPSE inhibitors such as free HS or proteins with HS side chains. It is known that circulating syndecan–1 levels are increased during acute PUUV–HFRS [36].

We hypothesized that the increased urinary HPSE levels in PUUV–HFRS could be due to a local increase in the enzyme by the direct viral infection of renal cells. We selected podocytes as our cell culture model due to their known susceptibility to orthohantaviral infection [18,51] and possible causative link to proteinuria in PUUV–HFRS [19], as well as their propensity to increase HPSE production in response to proteinuria–promoting factors such as glucose [43,44]. As our orthohantavirus model virus, we used HTNV, which causes more severe HFRS as compared to PUUV and is more readily grown to high titers in cell culture. We observed that a high initial dose of HTNV (MOI 10) was able to induce increased HPSE levels and mRNA expression in podocytes, which was due to its ability to efficiently replicate (UV–inactivated virus did not show the same effect) in podocytes during the timeframe set up for our experiment. With a lower infectious dose of HTNV (MOI 1), no infection was observed during the 4 dpi, which is in line with the slow infection kinetics of orthohantaviruses in podocytes [18,51,52]. We also carried out PUUV infections in podocytes, but, due to the relatively low titers achieved for PUUV in cell culture, we were not able to replicate the high initial virus dose of HTNV and therefore could not detect sufficient infection by PUUV in our assay setup. The molecular mechanisms leading to increased expression of HPSE mRNA in infected podocytes are unclear but could involve increased expression of pro–inflammatory cytokines such as tumor necrosis factor α , which is known to induce HPSE [53] and is upregulated in acute PUUV–HFRS [54].

Our data indicate that an efficient old–world orthohantavirus infection of podocytes can result in increased HPSE secretion, which is likely to contribute to elevated HPSE levels in patient urine, possibly promoting endothelial cell permeability and proteinuria locally in patient kidneys by degrading endothelial glycocalyx HS chains, subsequently altering the GFB’s charge–selectivity. Whether increased HPSE levels, and thus activity, in infected podocytes could contribute to decreased podocyte motility and the disruption of cell–to–cell contacts, as observed by other investigators [18,51], remains to be determined. The extensive crosstalk between podocytes and glomerular endothelial cells is well known [55] and endothelial glycocalyx degradation would likely have adverse effects also on podocyte functions and could potentially lead to podocyte injury.

One of the limitations of this study was that syndecan–1 was not measured from plasma, since the employed ELISA assay did not show the required specificity in the plasma samples used for this study. In addition, although eGFR is accurate to assess kidney function during chronic kidney injury, its use during AKI is controversial because of its fast onset and resolution. However, we decided to use eGFR instead of plasma creatinine as an indication of AKI in this study, since it takes the gender and weight of the patients into account. Another clinical parameter describing disease severity in this study was minimum MAP. Hypotonic shock is the most common cause of death in the more severe forms of HFRS, but the patients included in this study did not suffer from hemodynamic failure or hypotonia and only 5 out of 56 patients had minimum MAP below 70 mmHg during hospital stay. This indicates that our patient cohort had a relatively mild course

of HFRS, which is typical for PUUV infections. Thus, while low MAP is not necessarily important for the pathogenesis of PUUV-caused HFRS, we feel that its prominence in the more severe forms of the disease justifies its inclusion as one of the clinical parameters in our analysis. This can hopefully indirectly provide insight into the possible role of the currently measured parameters, HPSE and syndecan-1, also in more severe HFRS. Furthermore, it needs to be added that podocytes are not necessarily the only source of HPSE in the kidneys during acute HFRS, and infected glomerular endothelial cells could also contribute to the overall HPSE levels.

5. Conclusions

Acute PUUV-HFRS presented with elevation of HPSE and syndecan-1 levels in urine. These urinary HPSE levels were strongly associated with overall disease severity and albuminuria. Moreover, multiple regression analyses revealed that urinary HPSE increases the predictive power on dependent variables such as MAP and urinary albumin. Finally, we demonstrated through in vitro assays that HTNV infection of podocytes led to the upregulation of HPSE. Therefore, HPSE activity is potentially upregulated during HFRS, which could be the cause of renal endothelium glycocalyx degradation. Further studies are needed on this topic, but these results point towards the potential use of HPSE inhibitors as therapeutic treatment options during acute HFRS.

Supplementary Materials: The following supporting information can be downloaded at: <https://www.mdpi.com/article/10.3390/v14030450/s1>, Figure S1. Spearman rank correlation coefficient matrix using absolute concentrations of variables measured from urine. The colors of the round circles indicate the level of the correlation coefficient and increasing size with a lower p -value. Statistical significance is specified as * = $p < 0.05$, ** = $p < 0.01$, *** = $p < 0.001$, **** = $p < 0.0001$. AOF = after onset of fever, LOS = length of stay, eGFR = estimated glomerular filtration rate, P = plasma, U = urine, crea = creatinine, alb = albumin, HPSE = heparanase, Synd-1 = syndecan-1, IL = interleukin, IP-10 = interferon gamma-induced protein 10, MCP-1 = monocyte chemoattractant protein-1, MAP = mean arterial pressure, WBC = white blood cells, MPO = myeloperoxidase, CRP = plasma C-reactive protein, tromb = thrombocytes.

Author Contributions: Conceptualization, L.E.C. and T.S.; methodology, L.E.C., T.S., S.M., J.M. and C.S.; validation, O.V., A.V., S.M. and J.M.; formal analysis, L.E.C. and T.S.; investigation, L.E.C. and C.S.; resources, T.S., M.A.S., S.L. and J.M.; data curation, L.E.C., T.S., J.M. and S.M.; writing—original draft preparation, L.E.C.; writing—review and editing, all authors; visualization, L.E.C.; supervision, T.S. and S.L.; project administration, T.S., O.V., A.V. and J.M.; funding acquisition, T.S. All authors have read and agreed to the published version of the manuscript.

Funding: This research was funded by the Academy of Finland (grant number 321809, to T.S.), Sigrid Jusélius Foundation (grant number MS568, to A.V. and J.M.), Magnus Ehrnrooth Foundation (to A.V.), Finnish Kidney Foundation/Munuaissäätiö (to L.E.C.), Competitive State Research Financing of the Expert Responsibility Area of Tampere University Hospital (grant numbers 9X033 and 9V040, to J.M. and S.M.) and Tampere Tuberculosis Foundation (grant number MS759, to J.M.).

Institutional Review Board Statement: The study was conducted in accordance with the Declaration of Helsinki and approved by the Ethics Committees of Tampere University Hospital (permit number R04180), which approved the use of patient samples.

Informed Consent Statement: Informed consent was obtained from all subjects involved in the study.

Data Availability Statement: Not applicable.

Acknowledgments: We thank Sanna Mäki and Päivi Yli-Nikkilä for the expert technical assistance. Open Access Funding provided by University of Helsinki.

Conflicts of Interest: The authors declare no conflict of interest. The funders had no role in the design of the study; in the collection, analyses, or interpretation of data; in the writing of the manuscript, or in the decision to publish the results.

References

1. Jonsson, C.B.; Figueiredo, L.T.; Vapalahti, O. A global perspective on hantavirus ecology, epidemiology, and disease. *Clin. Microbiol. Rev.* **2010**, *23*, 412–441. [[CrossRef](#)] [[PubMed](#)]
2. Vaehri, A.; Strandin, T.; Hepojoki, J.; Sironen, T.; Henttonen, H.; Mäkelä, S.; Mustonen, J. Uncovering the mysteries of hantavirus infections. *Nat. Rev. Microbiol.* **2013**, *11*, 539–550. [[CrossRef](#)]
3. Hepojoki, J.; Vaehri, A.; Strandin, T. The fundamental role of endothelial cells in hantavirus pathogenesis. *Front Microbiol.* **2014**, *22*, 727. [[CrossRef](#)]
4. Mustonen, J.; Outinen, T.; Laine, O.; Pörsti, I.; Vaehri, A.; Mäkelä, S. Kidney disease in Puumala hantavirus infection. *Infect. Dis.* **2017**, *49*, 321–332. [[CrossRef](#)] [[PubMed](#)]
5. Ala-Houhala, I.; Koskinen, M.; Ahola, T.; Harmoinen, A.; Kouri, T.; Laurila, K.; Mustonen, J.; Pasternack, A. Increased glomerular permeability in patients with nephropathia epidemica caused by Puumala hantavirus. *Nephrol. Dial. Transplant.* **2002**, *17*, 246–252. [[CrossRef](#)]
6. Mantula, P.; Tietäväinen, J.; Clement, J.; Niemelä, O.; Pörsti, I.; Vaehri, A.; Mustonen, J.; Mäkelä, S.; Outinen, T. Flash-Like Albuminuria in Acute Kidney Injury Caused by Puumala Hantavirus Infection. *Pathogens* **2020**, *9*, 615. [[CrossRef](#)]
7. Mantula, P.S.; Outinen, T.K.; Clement, J.P.G.; Huhtala, H.S.A.; Pörsti, I.H.; Vaehri, A.; Mustonen, J.T.; Mäkelä, S.M. Glomerular Proteinuria Predicts the Severity of Acute Kidney Injury in Puumala Hantavirus-Induced Tubulointerstitial Nephritis. *Nephron* **2017**, *136*, 193–201. [[CrossRef](#)] [[PubMed](#)]
8. Boehlke, C.; Hartleben, B.; Huber, T.B.; Hopfer, H.; Walz, G.; Neumann-Haefelin, E. Hantavirus infection with severe proteinuria and podocyte foot-process effacement. *Am. J. Kidney Dis.* **2014**, *64*, 452–456. [[CrossRef](#)]
9. Outinen, T.K.; Mäkelä, S.; Clement, J.; Paakkala, A.; Pörsti, I.; Mustonen, J. Community Acquired Severe Acute Kidney Injury Caused by Hantavirus-Induced Hemorrhagic Fever with Renal Syndrome Has a Favorable Outcome. *Nephron* **2015**, *130*, 182–190. [[CrossRef](#)] [[PubMed](#)]
10. Breshears, M.A.; Anthony, W.; Confer, A. *Pathologic Basis of Veterinary Disease*, 6th ed.; Elsevier: Amsterdam, The Netherlands, 2017.
11. Rostgaard, J.; Qvortrup, K. Sieve plugs in fenestrae of glomerular capillaries—Site of the filtration barrier? *Cells Tissues Organs* **2002**, *170*, 132–138. [[CrossRef](#)] [[PubMed](#)]
12. Curry, F.E.; Adamson, R.H. Endothelial glycocalyx: Permeability barrier and mechanosensor. *Ann. Biomed. Eng.* **2012**, *40*, 828–839. [[CrossRef](#)]
13. Avasthi, P.S.; Koshy, V. The anionic matrix at the rat glomerular endothelial surface. *Anat. Rec.* **1988**, *220*, 258–266. [[CrossRef](#)] [[PubMed](#)]
14. Kerjaschki, D.; Sharkey, D.J.; Farquhar, M.G. Identification and characterization of podocalyxin—The major sialoprotein of the renal glomerular epithelial cell. *J. Cell. Biol.* **1984**, *98*, 1591–1596. [[CrossRef](#)] [[PubMed](#)]
15. Ina, K.; Kitamura, H.; Nakamura, M.; Ono, J.; Takaki, R. Loss of sulfated carbohydrate from the glomerular podocyte as a cause of albuminuria in experimental diabetic rats: Ultrastructural histochemical study. *J. Diabet. Complications.* **1991**, *5*, 173–175. [[CrossRef](#)]
16. Menzel, S.; Moeller, M.J. Role of the podocyte in proteinuria. *Pediatr. Nephrol.* **2011**, *26*, 1775–1780. [[CrossRef](#)] [[PubMed](#)]
17. Krautkrämer, E.; Zeier, M.; Plyusnin, A. Hantavirus infection: An emerging infectious disease causing acute renal failure. *Kidney Int.* **2013**, *83*, 23–27. [[CrossRef](#)] [[PubMed](#)]
18. Krautkrämer, E.; Grouls, S.; Stein, N.; Reiser, J.; Zeier, M. Pathogenic old world hantaviruses infect renal glomerular and tubular cells and induce disassembling of cell-to-cell contacts. *J. Virol.* **2011**, *85*, 9811–9823. [[CrossRef](#)] [[PubMed](#)]
19. Nussag, C.; Stütz, A.; Hägele, S.; Speer, C.; Kälble, F.; Eckert, C.; Brenner, T.; Weigand, M.A.; Morath, C.; Reiser, J.; et al. Glomerular filtration barrier dysfunction in a self-limiting, RNA virus-induced glomerulopathy resembles findings in idiopathic nephrotic syndromes. *Sci. Rep.* **2020**, *10*, 19117. [[CrossRef](#)]
20. Cosgriff, T.M. Mechanisms of disease in Hantavirus infection: Pathophysiology of hemorrhagic fever with renal syndrome. *Rev. Infect. Dis.* **1991**, *13*, 97–107. [[CrossRef](#)] [[PubMed](#)]
21. Gelberg, H.; Healy, L.; Whiteley, H.; Miller, L.A.; Vimr, E. In vivo enzymatic removal of alpha 2—>6-linked sialic acid from the glomerular filtration barrier results in podocyte charge alteration and glomerular injury. *Lab. Invest.* **1996**, *74*, 907–920. [[PubMed](#)]
22. Jeansson, M.; Haraldsson, B. Glomerular size and charge selectivity in the mouse after exposure to glucosaminoglycan-degrading enzymes. *J. Am. Soc. Nephrol.* **2003**, *14*, 1756–1765. [[CrossRef](#)] [[PubMed](#)]
23. Jeansson, M.; Haraldsson, B. Morphological and functional evidence for an important role of the endothelial cell glycocalyx in the glomerular barrier. *Am. J. Physiol. Renal. Physiol.* **2006**, *290*, F111–6. [[CrossRef](#)] [[PubMed](#)]
24. Meuwese, M.C.; Broekhuizen, L.N.; Kuikhoven, M.; Heeneman, S.; Lutgens, E.; Gijbels, M.J.; Nieuwdorp, M.; Peutz, C.J.; Stroes, E.S.; Vink, H.; et al. Endothelial surface layer degradation by chronic hyaluronidase infusion induces proteinuria in apolipoprotein E-deficient mice. *PLoS ONE* **2010**, *5*, e14262. [[CrossRef](#)]
25. Dane, M.J.; van den Berg, B.M.; Avramut, M.C.; Faas, F.G.; van der Vlag, J.; Rops, A.L.; Ravelli, R.B.; Koster, B.J.; van Zonneveld, A.J.; Vink, H.; et al. Glomerular endothelial surface layer acts as a barrier against albumin filtration. *Am. J. Pathol.* **2013**, *182*, 1532–1540. [[CrossRef](#)]
26. Kanwar, Y.S.; Farquhar, M.G. Presence of heparan sulfate in the glomerular basement membrane. *Proc. Natl. Acad. Sci. USA* **1979**, *76*, 1303–1307. [[CrossRef](#)] [[PubMed](#)]

27. Kanwar, Y.S.; Farquhar, M.G. Isolation of glycosaminoglycans (heparan sulfate) from glomerular basement membranes. *Proc. Natl. Acad. Sci. USA* **1979**, *76*, 4493–4497. [[CrossRef](#)]
28. Kanwar, Y.S.; Linker, A.; Farquhar, M.G. Increased permeability of the glomerular basement membrane to ferritin after removal of glycosaminoglycans (heparan sulfate) by enzyme digestion. *J. Cell Biol.* **1980**, *86*, 688–693. [[CrossRef](#)]
29. Kanwar, Y.S.; Jakubowski, M.L.; Rosenzweig, L.J. Distribution of sulfated glycosaminoglycans in the glomerular basement membrane and mesangial matrix. *Eur. J. Cell. Biol.* **1983**, *31*, 290–295.
30. Thakkar, N.; Yadavalli, T.; Jaishankar, D.; Shukla, D. Emerging Roles of Heparanase in Viral Pathogenesis. *Pathogens* **2017**, *6*, 43. [[CrossRef](#)] [[PubMed](#)]
31. Jeansson, M.; Björck, K.; Tenstad, O.; Haraldsson, B. Adriamycin alters glomerular endothelium to induce proteinuria. *J. Am. Soc. Nephrol.* **2009**, *20*, 114–122. [[CrossRef](#)]
32. Rahbar, E.; Cardenas, J.C.; Baimukanova, G.; Usadi, B.; Bruhn, R.; Pati, S.; Ostrowski, S.R.; Johansson, P.I.; Holcomb, J.B.; Wade, C.E. Endothelial glyocalyx shedding and vascular permeability in severely injured trauma patients. *J. Transl. Med.* **2015**, *13*, 117. [[CrossRef](#)] [[PubMed](#)]
33. Rehm, M.; Bruegger, D.; Christ, F.; Conzen, P.; Thiel, M.; Jacob, M.; Chappell, D.; Stoeckelhuber, M.; Welsch, U.; Reichart, B.; et al. Shedding of the endothelial glyocalyx in patients undergoing major vascular surgery with global and regional ischemia. *Circulation* **2007**, *116*, 1896–1906. [[CrossRef](#)]
34. Rangarajan, S.; Richter, J.R.; Richter, R.P.; Bandari, S.K.; Tripathi, K.; Vlodaysky, I.; Sanderson, R.D. Heparanase–enhanced Shedding of Syndecan–1 and Its Role in Driving Disease Pathogenesis and Progression. *J. Histochem. Cytochem.* **2020**, *68*, 823–840. [[CrossRef](#)] [[PubMed](#)]
35. Teng, Y.H.; Aquino, R.S.; Park, P.W. Molecular functions of syndecan–1 in disease. *Matrix Biol.* **2012**, *31*, 3–16. [[CrossRef](#)] [[PubMed](#)]
36. Connolly–Andersen, A.M.; Thunberg, T.; Ahlm, C. Endothelial activation and repair during hantavirus infection: Association with disease outcome. *Open Forum Infect. Dis.* **2014**, *1*, ofu027. [[CrossRef](#)] [[PubMed](#)]
37. Levey, A.S.; Stevens, L.A.; Schmid, C.H.; Zhang, Y.L.; Castro, A.F., 3rd; Feldman, H.I.; Kusek, J.W.; Eggers, P.; Van Lente, F.; Greene, T.; et al. CKD–EPI (Chronic Kidney Disease Epidemiology Collaboration). A new equation to estimate glomerular filtration rate. *Ann. Intern. Med.* **2009**, *150*, 604–612. [[CrossRef](#)] [[PubMed](#)]
38. Buijssers, B.; Yanginlar, C.; de Nooijer, A.; Grondman, I.; Maciej–Hulme, M.L.; Jonkman, I.; Janssen, N.A.F.; Rother, N.; de Graaf, M.; Pickkers, P.; et al. Increased Plasma Heparanase Activity in COVID–19 Patients. *Front. Immunol.* **2020**, *11*, 575047. [[CrossRef](#)]
39. Libraty, D.H.; Mäkelä, S.; Vlk, J.; Hurme, M.; Vaheri, A.; Ennis, F.A.; Mustonen, J. The degree of leukocytosis and urine GATA–3 mRNA levels are risk factors for severe acute kidney injury in Puumala virus nephropathia epidemica. *PLoS ONE* **2012**, *7*, e35402.
40. Strandin, T.; Mäkelä, S.; Mustonen, J.; Vaheri, A. Neutrophil Activation in Acute Hemorrhagic Fever with Renal Syndrome Is Mediated by Hantavirus–Infected Microvascular Endothelial Cells. *Front. Immunol.* **2018**, *9*, 2098. [[CrossRef](#)]
41. Saleem, M.A.; O’Hare, M.J.; Reiser, J.; Coward, R.J.; Inward, C.D.; Farren, T.; Xing, C.Y.; Ni, L.; Mathieson, P.W.; Mundel, P. A conditionally immortalized human podocyte cell line demonstrating nephrin and podocin expression. *J. Am. Soc. Nephrol.* **2002**, *13*, 630–638. [[CrossRef](#)] [[PubMed](#)]
42. Schmittgen, T.D.; Livak, K.J. Analyzing real–time PCR data by the comparative C(T) method. *Nat. Protoc.* **2008**, *3*, 1101–1108. [[CrossRef](#)] [[PubMed](#)]
43. van den Hoven, M.J.; Waanders, F.; Rops, A.L.; Kramer, A.B.; van Goor, H.; Berden, J.H.; Navis, G.; van der Vlag, J. Regulation of glomerular heparanase expression by aldosterone, angiotensin II and reactive oxygen species. *Nephrol. Dial. Transplant.* **2009**, *24*, 2637–2645. [[CrossRef](#)] [[PubMed](#)]
44. Rabelink, T.J.; van den Berg, B.M.; Garsen, M.; Wang, G.; Elkin, M.; van der Vlag, J. Heparanase: Roles in cell survival, extracellular matrix remodelling and the development of kidney disease. *Nat. Rev. Nephrol.* **2017**, *13*, 201–212. [[CrossRef](#)] [[PubMed](#)]
45. Hoyer, J.R.; Seiler, M.W. Pathophysiology of Tamm–Horsfall protein. *Kidney Int.* **1979**, *16*, 279–289. [[CrossRef](#)] [[PubMed](#)]
46. Miettinen, M.H.; Makela, S.M.; Ala–Houhala, I.O.; Huhtala, H.S.; Koobi, T.; Vaheri, A.I.; Pasternack, A.I.; Porsti, I.H.; Mustonen, J.T. Tubular proteinuria and glomerular filtration 6 years after puumala hantavirus–induced acute interstitial nephritis. *Nephron Clin. Pract.* **2009**, *112*, c115–c120. [[CrossRef](#)] [[PubMed](#)]
47. Miettinen, M.H.; Mäkelä, S.M.; Ala–Houhala, I.O.; Huhtala, H.S.; Kööbi, T.; Vaheri, A.I.; Pasternack, A.I.; Pörsti, I.H.; Mustonen, J.T. Ten–year prognosis of Puumala hantavirus–induced acute interstitial nephritis. *Kidney Int.* **2006**, *69*, 2043–2048. [[CrossRef](#)] [[PubMed](#)]
48. Van den Hoven, M.J.; Rops, A.L.; Vlodaysky, I.; Levidiotis, V.; Berden, J.H.; Van der Vlag, J. Heparanase in glomerular diseases. *Kidney Int.* **2007**, *72*, 543–548. [[CrossRef](#)] [[PubMed](#)]
49. Szymczak, M.; Kuźniar, J.; Klinger, M. The role of heparanase in diseases of the glomeruli. *Arch. Immunol. Ther. Exp.* **2010**, *58*, 45–56. [[CrossRef](#)] [[PubMed](#)]
50. Shafat, I.; Ilan, N.; Zoabi, S.; Vlodaysky, I.; Nakhoul, F. Heparanase levels are elevated in the urine and plasma of type 2 diabetes patients and associate with blood glucose levels. *PLoS ONE* **2011**, *6*, e17312. [[CrossRef](#)] [[PubMed](#)]
51. Hägele, S. Functional Consequences of Old World Hantavirus Infection in Human Renal Cells. Ph.D. Thesis, Heidelberg University, Heidelberg, Germany, 2018. [[CrossRef](#)]
52. Hägele, S.; Müller, A.; Nusschag, C.; Reiser, J.; Zeier, M.; Krautkrämer, E. Virus– and cell type–specific effects in orthohantavirus infection. *Virus Res.* **2019**, *260*, 102–113. [[CrossRef](#)] [[PubMed](#)]

53. Chen, G.; Wang, D.; Vikramadithyan, R.; Yagy, H.; Saxena, U.; Pillarisetti, S.; Goldberg, I. Inflammatory Cytokines and Fatty Acids Regulate Endothelial Cell Heparanase Expression. *Biochemistry* **2004**, *43*, 4971–4977. [[CrossRef](#)] [[PubMed](#)]
54. Linderholm, M.; Ahlm, C.; Settergren, B.; Waage, A.; Tärnvik, A. Elevated Plasma Levels of Tumor Necrosis Factor (TNF)- α , Soluble TNF Receptors, Interleukin (IL)-6, and IL-10 in Patients with Hemorrhagic Fever with Renal Syndrome. *J. Infect. Dis.* **1996**, *173*, 38–43. [[CrossRef](#)] [[PubMed](#)]
55. Mahtal, N.; Lenoir, O.; Tharaux, P.L. Glomerular Endothelial Cell Crosstalk With Podocytes in Diabetic Kidney Disease. *Front. Med.* **2021**, *8*, 659013. [[CrossRef](#)] [[PubMed](#)]